

This discussion paper is/has been under review for the journal Atmospheric Chemistry and Physics (ACP). Please refer to the corresponding final paper in ACP if available.

## Variability of the Brewer-Dobson circulation

T. Flury et al.

# Variability of the Brewer-Dobson circulation's meridional and vertical branch using Aura/MLS water vapor

T. Flury<sup>1</sup>, D. L. Wu<sup>2</sup>, and W. G. Read<sup>1</sup>

<sup>1</sup>Jet Propulsion Laboratory, California Institute of Technology, Pasadena, California, USA

<sup>2</sup>NASA-Goddard Space Flight Center, Greenbelt, Maryland, USA

Received: 17 July 2012 – Accepted: 12 August 2012 – Published: 21 August 2012

Correspondence to: T. Flury (thomas.flury@jpl.nasa.gov)

Published by Copernicus Publications on behalf of the European Geosciences Union.

[Title Page](#)

[Abstract](#)

[Introduction](#)

[Conclusions](#)

[References](#)

[Tables](#)

[Figures](#)

[⏪](#)

[⏩](#)

[◀](#)

[▶](#)

[Back](#)

[Close](#)

[Full Screen / Esc](#)

[Printer-friendly Version](#)

[Interactive Discussion](#)



## Abstract

We use Aura/MLS stratospheric water vapor measurements to infer interannual variations in the speed of the Brewer-Dobson circulation (BDC) from 2004 to 2011. Stratospheric water vapor ( $\text{H}_2\text{O}$ ) is utilized as a tracer for dynamics and we follow its path along the vertical and meridional branch of the BDC from the tropics to mid-latitudes. We correlate one year time series of  $\text{H}_2\text{O}$  in the lower stratosphere at two subsequent altitude levels (68 hPa,  $\sim 18.8$  km and 56 hPa,  $\sim 19.9$  km at the Equator) and determine the time lag for best correlation. The same calculation is made on the horizontal on the 100 hPa ( $\sim 16.6$  km) level by correlating the  $\text{H}_2\text{O}$  time series at the Equator with the ones at  $40^\circ\text{N}$  and  $40^\circ\text{S}$ . From these lag coefficients we derive the vertical and horizontal speeds of the BDC in the tropics and extra-tropics respectively. We observe a clear interannual variability of the vertical and horizontal branch. The variability reflects signatures of the Quasi Biennial Oscillation (QBO). Our measurements confirm the QBO meridional circulation anomalies and show that the speed variations in the two branches of the BDC are out of phase and fairly well anti-correlated. Maximum ascent rates are found during the QBO easterly phase. We also find that the transport towards the Northern Hemisphere (NH) is on the average two times faster than to the Southern Hemisphere (SH) with a mean speed of  $1.15\text{ m s}^{-1}$  at 100 hPa. Furthermore, the speed towards the NH shows much more variability with an amplitude of about 21 % whilst the speed towards the SH varies by only 10 %. An amplitude of 21 % is also observed in the variability of the ascent rate at the Equator which is on the average  $0.2\text{ mm s}^{-1}$  and hence about 5000 times slower than the meridional branch.

## 1 Introduction

The very low amounts of water vapor ( $\text{H}_2\text{O}$ ) measured in the lower stratosphere by Brewer (1949) implied that air masses must be entering the stratosphere through the cold tropical tropopause because nowhere else temperatures are low enough to allow

ACPD

12, 21291–21320, 2012

### Variability of the Brewer-Dobson circulation

T. Flury et al.

Title Page

Abstract

Introduction

Conclusions

References

Tables

Figures

◀

▶

◀

▶

Back

Close

Full Screen / Esc

Printer-friendly Version

Interactive Discussion



## Variability of the Brewer-Dobson circulation

T. Flury et al.

Title Page

Abstract

Introduction

Conclusions

References

Tables

Figures

◀

▶

◀

▶

Back

Close

Full Screen / Esc

Printer-friendly Version

Interactive Discussion



for sufficient dehydration. Dobson (1956) used ground-based measurements of total ozone and observed minimum values in the photo-chemical source region of the tropics and maximum values in the extra-tropics. Hence, he assumed a transport from the tropical stratosphere towards the pole in both hemispheres marked by low-latitude ascent and high-latitude descent. The assumption of a poleward residual circulation now called Brewer-Dobson circulation (BDC) is still valid today. Figure 1 shows the different branches of the BDC (adapted from Plumb (2002)). Air masses ascend inside the tropical pipe, which represents a mixing barrier for tropical and extra-tropical air (Plumb, 1996). The rising air is distributed symmetrically toward both hemispheres in the lowermost stratosphere (black arrows) and brings H<sub>2</sub>O from low- to high-latitudes. However, in the upper stratosphere air masses are predominantly directed toward the winter pole where they mix and descend into the so called surf zone and the polar vortex. Stratospheric air returns to the troposphere at higher latitudes and is ultimately brought back into the tropics (equatorward arrows inside troposphere), where they join the tropospheric Hadley-cell with upwelling in the tropics and descent in the subtropics to form the subtropical ridge. Haynes et al. (1991) explained that the BDC is driven by breaking of high-latitude vertically propagating planetary and gravity waves which slow down the stratospheric zonal mean flow and induce a meridional residual circulation. The planetary wave breaking occurs mainly in the surf zone depicted in Fig. 1.

Randel et al. (2002a,b), Ueyama and Wallace (2010) and Dhomse et al. (2008) showed direct evidence of the correlation of high-latitude planetary wave breaking (mid-latitude eddy heat flux as a proxy) and the strength of the BDC. A stronger BDC leads to lower tropical tropopause temperatures (Randel et al., 2006) and to stronger freeze drying of the stratosphere (Dhomse et al., 2008) i.e. lower H<sub>2</sub>O concentrations. Knowledge of the BDC is thus crucial to determine the budget of H<sub>2</sub>O and other atmospheric trace gases in the stratosphere since it has an important influence on the stratospheric entry, the residence time and ozone depletion. The BDC has been varying since the 1960s (Roscoe, 2006). General circulation models (GCM) predict that in a warmer climate the mass exchange between the tropics and extra-tropics will increase (Butchart

et al., 2006; McLandress and Shepherd, 2009; Okamoto et al., 2011). The predicted enhancement of the BDC is due to an increase in planetary wave drag in the extratropical stratosphere. A change in the BDC will in turn also affect stratospheric H<sub>2</sub>O and ozone abundance.

5 Observational studies about the BDC variability are rare. Engel et al. (2009) showed by using balloon-borne measurements of stratospheric trace gases that the stratospheric mean age of air was slightly increasing rather than decreasing. This result disagrees with model predictions for a strengthening of the BDC and an associated decrease in the mean age of air. By using Aura/MLS measurements of H<sub>2</sub>O we derive  
10 the average speed of the BDC's vertical branch in the tropics as well as the meridional branch towards the mid-latitudes near 100 hPa which are highlighted by the thick blue and black arrows in Fig. 1. Flury et al. (2012) showed that total water (ice & vapor) is roughly constant in the tropical tropopause layer (TTL) at 100 hPa on seasonal time scales. However, the temperature determines the balance between ice in cirrus clouds and water vapor. Thus, the strong seasonal cycle of temperature manifests itself also  
15 in water vapor and ice and can be found in water vapor throughout the lower stratosphere from tropics to mid-latitudes due to transport by the BDC. The slow transport of air out of the lower tropical stratosphere leads to a time lag in the H<sub>2</sub>O time series at higher latitudes and altitudes because lower stratospheric H<sub>2</sub>O is set in the tropics.  
20 This time lag enables us to retrieve the average speed of the BDC thanks to the tracer characteristics of H<sub>2</sub>O.

Several previous studies used the H<sub>2</sub>O tape recorder signal to derive the ascent rate in the tropical lower stratosphere (Mote et al., 1996; Schoeberl et al., 2008; Niwano et al., 2003; Fujiwara et al., 2010). The tropical H<sub>2</sub>O tape recorder is displayed in Fig. 2 and shows the imprinted seasonal cycle of H<sub>2</sub>O around the 100 hPa level which is then transported upward by the slow BDC ascent. Fujiwara et al. (2010) and Niwano et al. (2003) showed the seasonality and a clear modulation of the ascent rate by the Quasi Biennial Oscillation (QBO) using radiosonde measurements and HALOE satellite measurements, respectively. The QBO is a dynamic phenomenon in the equatorial strato-

## Variability of the Brewer-Dobson circulation

T. Flury et al.

Title Page

Abstract

Introduction

Conclusions

References

Tables

Figures

⏪

⏩

◀

▶

Back

Close

Full Screen / Esc

Printer-friendly Version

Interactive Discussion



**Variability of the  
Brewer-Dobson  
circulation**

T. Flury et al.

Title Page

Abstract

Introduction

Conclusions

References

Tables

Figures

◀

▶

◀

▶

Back

Close

Full Screen / Esc

Printer-friendly Version

Interactive Discussion



sphere and manifests itself by a quasi periodic oscillation ( $\cong 28$ -29 months) of the zonal wind between westerlies and easterlies. The alternating winds propagate downward from the stratopause (1 hPa,  $\sim 55$  km) at a rate of about 1 km per month towards the tropical tropopause (100 hPa,  $\sim 16.6$  km). The ascent rate of the tape recorder is modulated by the QBO and speeds up during the colder easterly phase and slows down during the warmer westerly phase (Niwano et al., 2003; Plumb and Bell, 1982). The ascent rate is thus anti-correlated with the temperature. As a consequence the strength of the BDC determines stratospheric H<sub>2</sub>O entry values by modulating TTL temperatures. The QBO affects also the meridional wind. In fact, it induces a secondary meridional circulation due to thermal wind balance, which affects the meridional branch of the BDC (Plumb and Bell, 1982; Baldwin et al., 2001; Ribera et al., 2004; Punge et al., 2009). More about the QBO can be found in Baldwin et al. (2001) and references therein.

Previous studies focused on the seasonal and interannual variations in the tropical ascending branch of the Brewer-Dobson circulation. We add observations of the speed of the meridional branch at 100 hPa and concentrate on the link between the vertical and the shallow meridional branch of the BDC as highlighted by the thick arrows in Fig. 1. We also investigate the difference between the Northern (NH) and Southern Hemisphere (SH) by considering the different amplitude of the QBO signal in the NH and SH. Furthermore, we link the derived speeds to temperature and zonal wind variability. The article is organized as follows. Section 2 describes the utilized satellite and reanalysis data as well as the correlation method. Section 3 outlines the results, especially the interannual speed variations and their link to temperature and zonal wind. Section 4 discusses the QBO's effect on the tropical pipe. Finally we conclude and summarize our findings in Sect. 5.

## 2 Data and method

In this study we analyze measurements from the MLS (Microwave Limb Sounder) instrument which is flown on board the Aura spacecraft and part of the NASA A-

train satellite constellation. MLS measurements began in August 2004 and continue since. We use daily mean H<sub>2</sub>O and temperature data of version 3.3. Approximately 3500 H<sub>2</sub>O profiles are retrieved on a daily basis from 316 hPa to 0.0002 hPa between 82° S and 82° N. MLS has a horizontal resolution of 200–300 km along track, 7 km across track and 3–4 km in the vertical. In this study we will focus on the lower stratospheric pressure levels of 100 hPa, 82 hPa, 68 hPa, 56 hPa, 46 hPa, 38 hPa, 32 hPa, 26 hPa, 22 hPa and 18 hPa. The precision and accuracy of H<sub>2</sub>O at 100 hPa is 10 % and 8 % respectively (Read et al., 2007). The MLS temperature product is retrieved from 316 hPa to 0.001 hPa and interpolated on the same horizontal grid as H<sub>2</sub>O for the purpose of the study. It has a vertical resolution of about 5 km at 100 hPa decreasing to 3 km in the middle stratosphere. The precision at 100 hPa is 0.8 K whilst the uncertainty is about 2 K (warm bias to other instruments such as CHAMP and AIRS/AMSU Schwartz et al. (2008)). To compare our observations with the QBO we use the National Centers for Environmental Prediction/National Center for Atmospheric Research (NCEP/NCAR) reanalysis daily zonal wind data, which are retrieved on 17 pressure levels from 1000 hPa to 10 hPa. The method used to determine vertical and meridional speeds of the BDC is similar to the one introduced by Schoeberl et al. (2008) and Flury et al. (2012). We calculate the time lagged correlation in the H<sub>2</sub>O time series between two different levels. The average speed is then determined by the ratio of the distance between the two levels and the calculated optimal time lag. In order to obtain a time series of the average speed we use a one year time window for correlation and shift one level in time with respect to the other until a maximum correlation is reached. In choosing such a 1 yr time window for correlation we concentrate on inter-annual variations. This correlation procedure is repeated every day until the end of the measurement time series. Thus, each daily value of the derived speed time series represents the average speed over the following 365 days. For the vertical speed we focus on the 68 hPa and 56 hPa level at the Equator which are separated on the average by 1.12 km. The distance between the two pressure levels is determined with the MLS version 3.3 geopotential height data (Schwartz et al., 2008), which were averaged over

**Variability of the  
Brewer-Dobson  
circulation**

T. Flury et al.

Title Page

Abstract

Introduction

Conclusions

References

Tables

Figures

◀

▶

◀

▶

Back

Close

Full Screen / Esc

Printer-friendly Version

Interactive Discussion



the respective time period of interest. We choose this altitude to make sure to be completely above tropical convection. To determine the speed of the meridional branch we correlate the 100 hPa levels at the Equator and 40° latitude North and South. We focus on the 100 hPa level because above 68 hPa H<sub>2</sub>O loses its distinctive tracer capabilities towards the mid-latitudes due to the so called tropical pipe which is a strong tropical mixing barrier (Plumb, 1996). We estimate the uncertainty of the derived speeds to be 5%. The main contributor is the uncertainty in the determination of the optimal time lag, which is about 2 days in the here shown analysis.

### 3 Results

#### 3.1 Water vapor transport

Due to its long chemical lifetime of the order of tens of years in the lower stratosphere (Bresseur and Solomon, 2005) H<sub>2</sub>O can be used as a tracer for atmospheric transport in that region. Vertical transport mechanisms can be visualized with the time series of tropical zonal mean H<sub>2</sub>O profiles. Figure 2 shows the well known atmospheric tape recorder (Mote et al., 1996) as the pressure-time series of H<sub>2</sub>O deviations from its time mean at each pressure level. The seasonal cycle of H<sub>2</sub>O at 100 hPa is imprinted and transported upward by the ascending branch of the BDC highlighted by the arrow. The signal is visible up to 10 hPa. Short term interannual variations in H<sub>2</sub>O are produced by the QBO and El Niño Southern Oscillation (ENSO). The irregular interannual variability between 200 hPa and 100 hPa follows the ENSO signal. During El Niño the atmosphere is warmer and carries more H<sub>2</sub>O (red) e.g. in 2005, 2007 and 2010. A strong La Niña occurred in 2007–2008 and 2010–2012 where H<sub>2</sub>O is well below the average (blue). The variable speed of the ascending air masses can be estimated by computing the slope of the alternating colored surfaces above 100 hPa highlighted by the arrow.

Figure 3 shows latitude-time series of H<sub>2</sub>O deviations from its zonal mean at 100 hPa. The seasonal cycle is clearly visible over the whole latitude range. Red colors represent

## Variability of the Brewer-Dobson circulation

T. Flury et al.

Title Page

Abstract

Introduction

Conclusions

References

Tables

Figures



Back

Close

Full Screen / Esc

Printer-friendly Version

Interactive Discussion



higher than average H<sub>2</sub>O whilst blue is below the average. Furthermore, we observe that the alternating bands of positive (red) and negative (blue) H<sub>2</sub>O anomalies are transported towards the high-latitudes which is highlighted by the two arrows which represent the shallow meridional branch of the BDC as previously shown in Fig. 1 by the two thick black vectors. The arrow is steeper in the NH which means a faster transport, hence a stronger BDC. The negative anomalies at high southern latitudes in the second half of each year stem from the very cold Antarctic polar vortex and the buildup of polar stratospheric clouds which dehydrate the 100 hPa level.

### 3.2 BDC speed variations

To compute the average speed of the vertical and meridional branch of the BDC as highlighted by the thick arrows in Fig. 1, we correlate the time series of the 68 hPa (~18.80 km) and 56 hPa (~19.92 km) level in one year windows over the whole MLS time series. Correlation is strong with coefficients  $r > 0.9$ . Since the tape recorder signal is ascending, the H<sub>2</sub>O at 56 hPa is lagged in time with the one at the lower level. We determine this time lag in order to get maximum correlation between the two levels. The optimal time lag determines the average time it takes for an air parcel to ascend by one MLS pressure level, thus the ascent rate can be computed from the ratio of the mean distance between the two levels ( $\Delta z \sim 1.12$  km) and the time lag. The same calculation is done for the meridional transport, which constitutes the shallow branch of the BDC. We compute the time lagged correlation between the 100 hPa levels at the Equator and 40° N and 40° S ( $\Delta y \sim 4440$  km). Correlation coefficients are also generally  $r > 0.9$ . The uncertainty of the method is composed of the uncertainty in the distance between the levels (~2%) and the precision of the time lag determination ( $\sim \pm 2$  day). The two sum up to about 5% uncertainty in the derived speed which is significantly smaller than the interannual variability of 21% found in the study. Figure 4 shows the results of the mean vertical and horizontal speeds of the BDC derived from the correlation of H<sub>2</sub>O time series. Note that the speed  $v$  in both hemispheres is taken positive towards either pole. The meridional transport in the NH ( $v$ , NH on the order of  $1 \text{ m s}^{-1}$ ) is about 5700

## Variability of the Brewer-Dobson circulation

T. Flury et al.

Title Page

Abstract

Introduction

Conclusions

References

Tables

Figures

◀

▶

◀

▶

Back

Close

Full Screen / Esc

Printer-friendly Version

Interactive Discussion



times faster than the vertical ascent ( $w$ ) which is  $\sim 0.2 \text{ mm s}^{-1}$ . The speed towards the SH ( $v$ , SH) is about half the one in the NH, which confirms the findings of Fig. 3. Also the variability of about 10 % is half the variability in the NH (21 %). The variability in the vertical ascent ( $\sim 21$  %) is very similar to the one in the meridional to the NH. There is a prominent  $\sim 2$  yr oscillation in  $v$ , NH and  $w$  which is linked to the QBO. However, an intriguing observation is the anti-correlation between the speeds of the two BDC branches in the NH. When the vertical branch speeds up, the meridional slows down. Both branches build the Brewer-Dobson circulation but show opposite interannual variations. Section 3.4 will discuss these findings in more detail.

Since we use one year increments of  $\text{H}_2\text{O}$  data for correlation we do not get the typical seasonal variation of the Brewer-Dobson circulation which is picking up in the months September to March every year due to enhanced high-latitude stratospheric wave breaking. Niwano et al. (2003) showed time series of vertical ascent rate profiles using HALOE  $\text{H}_2\text{O}$  and  $\text{CH}_4$  data where the seasonal cycle is visible with maxima occurring during NH winter. To verify the Niwano et al. (2003) results we determine the time it takes for an air parcel to ascend by one pressure level using MLS daily zonal mean  $\text{H}_2\text{O}$  data averaged between  $8^\circ \text{ S}$ – $8^\circ \text{ N}$ . We are specifically investigating the time it takes to shift up a lower stratospheric segment of a profile by one MLS pressure level as can be identified in Fig. 5. Thereby we determine the number of days  $j$  it takes to obtain the best correlation of the 100 hPa to 56 hPa profile at time  $t_j$  with a profile taken one MLS pressure level higher up i.e. from 82 hPa to 46 hPa at a time  $t_{j+j}$ . This calculation is repeated for every day and subsequent pressure levels up to 10 hPa in order to get a time series of the average vertical ascent rate profile at a higher temporal resolution. We use MLS geopotential height data to compute the average height difference between the considered levels. The increasing spacing with altitude between the levels shown in Fig. 6 (from  $\Delta z = 1.11 \text{ km}$  to  $\Delta z = 1.31 \text{ km}$ ) is taken into consideration. The ascent rate is thus derived by the covered distance divided by the computed time lag. The speed is attributed to the center pressure level of the considered altitude layer. Figure 6 shows the time series of ascent rate profiles in the lower stratosphere

## Variability of the Brewer-Dobson circulation

T. Flury et al.

[Title Page](#)[Abstract](#)[Introduction](#)[Conclusions](#)[References](#)[Tables](#)[Figures](#)[◀](#)[▶](#)[◀](#)[▶](#)[Back](#)[Close](#)[Full Screen / Esc](#)[Printer-friendly Version](#)[Interactive Discussion](#)

between 68 hPa ( $\sim 18.8$  km) and 18 hPa ( $\sim 27.2$  km). The speed varies between about  $0.1 \text{ mm s}^{-1}$  and  $0.5 \text{ mm s}^{-1}$  with maximum values occurring usually during the NH autumn and winter months when the BDC is stronger. Maximum values increase with altitude which agrees with results of Niwano et al. (2003) and Schoeberl et al. (2008).

5 The values are greater than those obtained with the previous method because of the better time resolution. The average speed in the considered altitude range is about  $0.24 \text{ mm s}^{-1}$  which again compares well to Figure 4 taking into account the small increase of speed with altitude. However, to better compare the data with the vertical speed shown in Fig. 4 we compute the anomalies by removing the seasonal cycle which is shown in Fig. 7. Again, we observe a strong QBO signal which slowly descends with a speed of about  $1\text{--}1.5 \text{ km month}^{-1}$ . Lower ascent rates are observed in 2006, 2008 and 2010–2011. The variability of about 50% is bigger than observed in Fig. 4 and is due to the different method used to compute the speed.

### 3.3 Link of temperature and vertical ascent

15 The speed of the BDC circulation plays a key role in steering the tropical tropopause temperature as well as the temperature in the lower stratosphere. An increase in speed of the BDC leads to a cooling of the tropical tropopause and the stratosphere as was already shown by Niwano et al. (2003); Randel et al. (2006); Yulaeva et al. (1994). Triggered by enhanced upwelling, the reaction of the temperature is a combination of  
20 adiabatic cooling and ozone decrease due to advection of lower ozone concentrations from below (Yulaeva et al., 1994; Randel et al., 2006). Less ozone results in less radiative heating. In order to compare our time series of the ascent rate (see Figure 4) with the temperature anomalies at the same latitude and pressure we need to compute a moving average over a one year period since the calculated speeds represent the average over the following year. Figure 8 shows the time series of the MLS temperature anomaly at the Equator and 68 hPa smoothed by a one year forward moving average in blue and the ascent rate in dashed black. Each point in the time series represents thus  
25 the average over the next year. As expected, an increase of the vertical velocity is ac-

## Variability of the Brewer-Dobson circulation

T. Flury et al.

Title Page

Abstract

Introduction

Conclusions

References

Tables

Figures



Back

Close

Full Screen / Esc

Printer-friendly Version

Interactive Discussion



accompanied by a decrease in temperature. Clearly visible again is the QBO modulation producing the  $\sim 2$  yr cycle. The expected anti-correlation between the temperature and the vertical ascent can be seen as a validation of our method to compute the speed of the BDC.

### 3.4 QBO influence on BDC

The QBO is associated with a secondary meridional circulation anomaly that does not only affect the transport to the mid-latitudes but also the vertical ascent (Reed, 1964; Plumb and Bell, 1982; Choi et al., 2002; Punge et al., 2009; Ribera et al., 2004). Figure 9 shows schematically the QBO associated circulation anomaly as a latitude-height section on the left and the vertical profile of the equatorial zonal wind  $u$  on the right. Below the maximum easterlies (E) there is enhanced vertical ascent inside the easterly shear zone (EZX), which is associated with lower temperatures. At the altitude of maximum easterlies (E) we find meridional divergence towards the poles. Inside the westerly shear zone (WSZ) just below the maximum westerlies (W) we find a descent anomaly, which is associated with higher temperatures and slows the vertical ascent down. At the height of maximum westerlies we find a meridional convergence zone at the Equator. We adapted the sketch from Choi et al. (2002) and Punge et al. (2009) who drew two symmetrical cells separated by the Equator. However, Peña-Ortiz et al. (2008) report on an asymmetry in autumn and spring when there is only one cell which is shifted completely into the winter hemisphere. Our results also suggest an asymmetry in the meridional components since the interannual variability of the meridional branch towards the NH is twice as strong as to the SH (see Fig. 4). For this reason we adapted the size of the meridional arrows to highlight the asymmetry. To sum up, easterly winds are associated with cold anomalies and higher vertical ascent rates below the level of maximum easterlies whilst westerly winds are associated with warm anomalies and lower vertical ascent rates below the level of maximum westerlies.

To compare the theory of Fig. 9 with MLS measurements we compare the ascent rate with the zonal wind of a level higher up. In our case we choose the ascent rate

## Variability of the Brewer-Dobson circulation

T. Flury et al.

Title Page

Abstract

Introduction

Conclusions

References

Tables

Figures



Back

Close

Full Screen / Esc

Printer-friendly Version

Interactive Discussion



calculated between the levels 68 hPa and 56 hPa and the average zonal wind at the 32 hPa level, both time series are taken at the Equator. The results are displayed in Fig. 10. The ascent rate is plotted in black (dashed) and varies between  $0.14 \text{ mm s}^{-1}$  and  $0.24 \text{ mm s}^{-1}$ . The NCEP average zonal wind (solid blue) is anti-correlated ( $r = -0.84$ ) with the ascent rate and confirms the schematics of Fig. 9. The ascent rate starts increasing during the westerlies and decreases after the maximum easterlies are reached. The upward motion is slowest during the westerly wind regime. Note that even during the westerlies the ascent rate is positive, the red downward arrow in Fig. 9 only indicates the QBO induced anomaly which slows down the prevailing upward motion but does not reverse it.

Figure 11 shows the same zonal wind time series as in the previous figure but together with the average meridional speed between the Equator and  $40^\circ \text{ N}$  at 100 hPa. The zonal wind speed correlates with the meridional speed, the correlation coefficient here is  $r = 0.73$ . This behavior can also be explained with the drawing in Fig. 9. The considered 100 hPa level for meridional transport is well below the 32 hPa of the zonal wind and e.g. in the case of maximal eastward wind (E in Fig. 9) the converging arrows in the lowest part of the figure apply which slow down the transport towards the poles. During the westerly phase the meridional transport gets faster below, which also applies to our case here.

## 4 Discussion

We derived the speed of the vertical and meridional branch of the BDC in the tropics and extra-tropics respectively. We found that the QBO has a significant influence on the two branches affecting them in opposite ways. Below the zone of maximum easterlies (QBO east) the vertical speed increases and the meridional speed decreases. The opposite happens below the zone of maximum westerlies (QBO west) as suggested by Fig. 9. Thus the QBO influences how the upwelling air masses are distributed into the tropical stratosphere. We therefore suggest an influence on the tropical pipe (Plumb,

### Variability of the Brewer-Dobson circulation

T. Flury et al.

Title Page

Abstract

Introduction

Conclusions

References

Tables

Figures



Back

Close

Full Screen / Esc

Printer-friendly Version

Interactive Discussion



1996) to explain the variability of the speed towards the mid-latitudes. The tropical pipe is a mixing barrier in the stratosphere that separates tropical- from mid-latitude air which can be seen in steep gradients of various trace gas distributions such as e.g.  $N_2O$  and  $H_2O$ . The pipe is more pronounced above 20 km altitude than below. Figure 12 sketches the tropical pipe and BDC transport for the QBO easterly phase on the left and the QBO westerly phase on the right. We assume a constant vertical supply of tropospheric air that crosses the tropical tropopause during both QBO phases. The enhancement of the respective branches is highlighted by the increased and gray shaded arrows. During the easterly phase the meridional speed towards the NH is about 40 % smaller than during west. We suggest that during this time the tropical pipe is stronger and mixing with the mid-latitudes takes more time. On the other hand for continuity reasons the vertical ascent rate is increased by about 40 % (see Fig. 4) compared to the west phase. However, during the QBO westerly phase we observe the opposite, meridional transport is faster and vertical speed decreases. We thus assume that the tropical pipe is more leaky and allows for faster transport towards the mid-latitudes which in turn reduces the vertical speed because the increased meridional flux leaves less mass to be moved upward.

## 5 Conclusions

We obtained the average speed of the vertical and meridional branch of the Brewer-Dobson circulation from 7 yr of Aura/MLS stratospheric water vapor measurements. Since  $H_2O$  in the lower stratosphere is a good tracer for atmospheric transport we derive the speed of the BDC by computing the time lag for best correlation of  $H_2O$  time series at different levels. We found that the interannual variability of the BDC speed depends on the phase of the QBO. The vertical branch as well as the meridional branch towards the NH show amplitudes of about 21 % whereas the SH meridional branch is more constant. Moreover we found that the variability in the meridional (NH) and vertical branch are anti-correlated. This anti-correlation is regulated by the so called

### Variability of the Brewer-Dobson circulation

T. Flury et al.

Title Page

Abstract

Introduction

Conclusions

References

Tables

Figures



Back

Close

Full Screen / Esc

Printer-friendly Version

Interactive Discussion



QBO secondary meridional circulation which is sketched in Fig. 9. We suggest that during the QBO easterly phase the tropical pipe is stronger and it takes more time for tropical air masses to mix into mid-latitude air. However, during the QBO westerly phase the tropical pipe appears more leaky and meridional transport is faster.

5 MLS temperature measurements confirm the anti-correlation between temperatures and vertical speed and show cooling (warming) during the easterly (westerly) shear phase while vertical speed is higher (lower) and meridional speed is lower (higher) (Fig. 8). NCEP/NCAR zonal wind reanalysis data also show the influence of the QBO on the vertical and meridional branch of the BDC. Strong easterlies lead to faster vertical ascent whilst westerlies slow the ascent (Fig. 10). On the other hand westerlies higher up increase the meridional speed at the 100 hPa level whereas it is lower during the easterly phase (Fig. 11). However, since the QBO secondary meridional circulation is a function of altitude and time the conclusions derived here are based largely on MLS observations at 100 hPa and 68 hPa. We suggest that further studies concentrate on the meridional branch of the BDC higher up in the stratosphere using H<sub>2</sub>O and methane (CH<sub>4</sub>) data. H<sub>2</sub>O alone is less suitable as a tracer for horizontal transport above 68 hPa due to the oxidation of CH<sub>4</sub> which is a significant source of H<sub>2</sub>O in the stratosphere. The correct representation of the atmospheric tape recorder is an important test for a general circulation model. The underlying H<sub>2</sub>O distribution in the upper troposphere and the seasonal cycle is crucial for a correct representation, a task where most models still perform poorly as noted by Jiang et al. (2012). It is also difficult to find the QBO signal in the modeled tape recorder (J. Jiang, personal communication, 2012). MLS has been a very stable instrument for monitoring middle atmospheric dynamics though its primary strength is on atmospheric composition and chemistry. It is thus highly recommended to be used intensively for validation and improvements of global chemistry climate models since important atmospheric oscillations such as ENSO and QBO are well recorded by MLS measurements.

*Acknowledgements.* The research by TF and WGR was performed at Jet Propulsion Laboratory, California Institute of Technology under contract with NASA. TF was supported by the

## Variability of the Brewer-Dobson circulation

T. Flury et al.

Title Page

Abstract

Introduction

Conclusions

References

Tables

Figures



Back

Close

Full Screen / Esc

Printer-friendly Version

Interactive Discussion



Swiss National Science Foundation under grant PBBEP2\_133505 and the California Institute of Technology. DLW would like to acknowledge the support from the Aura project and the MLS team for making the H<sub>2</sub>O data available. Copyright 2012 California Institute of Technology. Government sponsorship acknowledged. Copyright 2012. All rights reserved.

## 5 References

- Baldwin, M. P., Gray, L. J., Dunkerton, T. J., Hamilton, K., Haynes, P. H., Randel, W. J., Holton, J. R., Alexander, M. J., Hirota, I., Horinouchi, T., Jones, D. B. A., Kinnerson, J. S., Marquardt, C., Sato, K., and Takahashi, M.: The quasi-biennial oscillation, *Rev. Geophys.*, 39, 179–230, doi:10.1029/1999RG000073, 2001. 21295
- 10 Brasseur, G. P. and Solomon, S.: *Aeronomy of the Middle Atmosphere: Chemistry and Physics of the Stratosphere and Mesosphere*, XII, 644 pp., 3rd rev. and enlarged ed. 1-4020-3284-6, Berlin, Springer, 2005. 21297
- Brewer, A. W.: Evidence for a world circulation provided by measurements of helium and water vapor distribution in the stratosphere, *Q. J. Roy. Meteor. Soc.*, 75, 351, doi:10.1002/qj.49707532603, 1949. 21292
- 15 Butchart, N., Scaife, A. A., Bourqui, M., de Grandpré, J., Hare, S. H. E., Kettleborough, J., Langematz, U., Manzini, E., Sassi, F., Shibata, K., Shindell, D., and Sigmond, M.: Simulations of anthropogenic change in the strength of the Brewer Dobson circulation, *Climate Dynamics*, 27, 727–741, doi:10.1007/s00382-006-0162-4, 2006. 21293
- 20 Choi, W., Lee, H., Grant, W. B., Park, J. H., Holton, J. R., Lee, K.-M., and Naujokat, B.: On the secondary meridional circulation associated with the quasi-biennial oscillation, *Tellus Series B Chemical and Physical Meteorology B*, 54, 395, doi:10.1034/j.1600-0889.2002.201286.x, 2002. 21301, 21317
- 25 Dhomse, S., Weber, M., and Burrows, J.: The relationship between tropospheric wave forcing and tropical lower stratospheric water vapor, *Atmos. Chem. Phys.*, 8, 471–480, doi:10.5194/acp-8-471-2008, 2008. 21293
- Dobson, G. M. G.: Origin and distribution of polyatomic molecules in the atmosphere., *Proc. R. Soc. Lond. A.*, 236, 187–193, 1956. 21293

## Variability of the Brewer-Dobson circulation

T. Flury et al.

Title Page

Abstract

Introduction

Conclusions

References

Tables

Figures

◀

▶

◀

▶

Back

Close

Full Screen / Esc

Printer-friendly Version

Interactive Discussion



## Variability of the Brewer-Dobson circulation

T. Flury et al.

Title Page

Abstract

Introduction

Conclusions

References

Tables

Figures

◀

▶

◀

▶

Back

Close

Full Screen / Esc

Printer-friendly Version

Interactive Discussion



- Engel, A., Möbius, T., Bönisch, H., Schmidt, U., Heinz, R., Levin, I., Atlas, E., Aoki, S., Nakazawa, T., Sugawara, S., Moore, F., Hurst, D., Elkins, J., Schauffler, S., Andrews, A., and Boering, K.: Age of stratospheric air unchanged within uncertainties over the past 30 years, *Nature Geosci.*, 2, 28–31, doi:10.1038/ngeo388, 2009. 21294
- 5 Flury, T., Wu, D. L., and Read, W. G.: Correlation among cirrus ice content, water vapor and temperature in the TTL as observed by CALIPSO and Aura/MLS, *Atmos. Chem. Phys.*, 12, 683–691, doi:10.5194/acp-12-683-2012, 2012. 21294, 21296
- Fujiwara, M., Vömel, H., Hasebe, F., Shiotani, M., Ogino, S.-Y., Iwasaki, S., Nishi, N., Shibata, T., Shimizu, K., Nishimoto, E., Valverde Canossa, J. M., Selkirk, H. B., and Oltmans, S. J.: Seasonal to decadal variations of water vapor in the tropical lower stratosphere observed with balloon-borne cryogenic frost point hygrometers, *J. Geophys. Res.*, 115, D18304, doi:10.1029/2010JD014179, 2010. 21294
- 10 Haynes, P. H., McIntyre, M. E., Shepherd, T. G., Marks, C. J., and Shine, K. P.: On the ‘Downward Control’ of Extratropical Diabatic Circulations by Eddy-Induced Mean Zonal Forces., *J. Atmos. Sci.*, 48, 651–680, doi:10.1175/1520-0469(1991)048<0651:OTCOED>2.0.CO;2, 1991. 21293
- Jiang, J. H., Su, H., Zhai, C., Perun, V. S., Del Genio, A., Nazarenko, L. S., Donner, L. J., Horowitz, L., Seman, C., Cole, J., Gettelman, A., Ringer, M. A., Rotstayn, L., Jeffrey, S., Wu, T., Brient, F., Dufresne, J.-L., Kawai, H., Koshiro, T., Watanabe, M., LÉcuyer, T. S., Volodin, E. M., Iversen, T., Drange, H., Mesquita, M. D. S., Read, W. G., Waters, J. W., Tian, B., Teixeira, J., and Stephens, G. L.: Evaluation of cloud and water vapor simulations in CMIP5 climate models using NASA A-Train satellite observations, *Journal of Geophysical Research (Atmospheres)*, 117, D14105, doi:10.1029/2011JD017237, 2012. 21304
- 20 McLandress, C. and Shepherd, T. G.: Simulated Anthropogenic Changes in the Brewer-Dobson Circulation, Including Its Extension to High Latitudes, *J. Climate*, 22, 1516, doi:10.1175/2008JCLI2679.1, 2009. 21294
- Mote, P. W., Rosenlof, K. H., McIntyre, M. E., Carr, E. S., Gille, J. C., Holton, J. R., Kinnery, J. S., Pumphrey, H. C., Russell III, J. M., and Waters, J. W.: An atmospheric tape recorder: The imprint of tropical tropopause temperatures on stratospheric water vapor, *J. Geophys. Res.*, 101, 3989–4006, doi:10.1029/95JD03422, 1996. 21294, 21297
- 30 Niwano, M., Yamazaki, K., and Shiotani, M.: Seasonal and QBO variations of ascent rate in the tropical lower stratosphere as inferred from UARS HALOE trace gas data, *J. Geophys. Res.*, 108, 4794, doi:10.1029/2003JD003871, 2003. 21294, 21295, 21299, 21300, 21313, 21314

## Variability of the Brewer-Dobson circulation

T. Flury et al.

Title Page

Abstract

Introduction

Conclusions

References

Tables

Figures

◀

▶

◀

▶

Back

Close

Full Screen / Esc

Printer-friendly Version

Interactive Discussion



Okamoto, K., Sato, K., and Akiyoshi, H.: A study on the formation and trend of the Brewer-Dobson circulation, *J. Geophys. Res.*, 116, D10117, doi:10.1029/2010JD014953, 2011. 21294

Peña-Ortiz, C., Ribera, P., García-Herrera, R., Giorgetta, M. A., and García, R. R.: Forcing mechanism of the seasonally asymmetric quasi-biennial oscillation secondary circulation in ERA-40 and MAECHAM5, *J. Geophys. Res.*, 113, D16103, doi:10.1029/2007JD009288, 2008. 21301

Plumb, A. R. and Bell, R. C.: A model of the quasi-biennial oscillation on an equatorial beta-plane, *Q. J. R. Meteorol. Soc.*, 108, 335–352, doi:10.1002/qj.49710845604, 1982. 21295, 21301, 21317

Plumb, R. A.: A “tropical pipe” model of stratospheric transport, *J. Geophys. Res.*, 101, 3957–3972, doi:10.1029/95JD03002, 1996. 21293, 21297, 21302

Plumb, R. A.: Stratospheric transport, *J. Meteorol. Soc. Jpn.*, 80, 793–809, 2002. 21293

Punge, H. J., Konopka, P., Giorgetta, M. A., and Müller, R.: Effects of the quasi-biennial oscillation on low-latitude transport in the stratosphere derived from trajectory calculations, *J. Geophys. Res.*, 114, D03102, doi:10.1029/2008JD010518, 2009. 21295, 21301, 21317

Randel, W. J., Garcia, R. R., and Wu, F.: Time-Dependent Upwelling in the Tropical Lower Stratosphere Estimated from the Zonal-Mean Momentum Budget., *J. Atmos. Sci.*, 59, 2141–2152, doi:10.1175/1520-0469(2002)059<2141:TDUITT>2.0.CO;2, 2002a. 21293

Randel, W. J., Wu, F., and Stolarski, R.: Changes in Column Ozone Correlated with the Stratospheric EP Flux, *J. Meteorol. Soc. Jpn.*, 80, 849–862, doi:10.2151/jmsj.80.849, 2002b. 21293

Randel, W. J., Wu, F., Vömel, H., Nedoluha, G. E., and Forster, P.: Decreases in stratospheric water vapor after 2001: Links to changes in the tropical tropopause and the Brewer-Dobson circulation, *J. Geophys. Res.*, 111, 12312, doi:10.1029/2005JD006744, 2006. 21293, 21300

Read, W. G., Lambert, A., Bacmeister, J., Cofield, R. E., Christensen, L. E., Cuddy, D. T., Daffer, W. H., Drouin, B. J., Fetzer, E., Froidevaux, L., Fuller, R., Herman, R., Jarnot, R. F., Jiang, J. H., Jiang, Y. B., Kelly, K., Knosp, B. W., Kovalenko, L. J., Livesey, N. J., Liu, H.-C., Manney, G. L., Pickett, H. M., Pumphrey, H. C., Rosenlof, K. H., Sabouchi, X., Santee, M. L., Schwartz, M. J., Snyder, W. V., Stek, P. C., Su, H., Takacs, L. L., Thurstans, R. P., Vömel, H., Wagner, P. A., Waters, J. W., Webster, C. R., Weinstock, E. M., and Wu, D. L.: Aura Microwave Limb Sounder upper tropospheric and lower stratospheric H<sub>2</sub>O and relative humidity

## Variability of the Brewer-Dobson circulation

T. Flury et al.

Title Page

Abstract

Introduction

Conclusions

References

Tables

Figures

◀

▶

◀

▶

Back

Close

Full Screen / Esc

Printer-friendly Version

Interactive Discussion

with respect to ice validation, *J. Geophys. Res.*, 112, D24S35, doi:10.1029/2007JD008752, 2007. 21296

Reed, R. J.: A tentative model of the 26-month oscillation in tropical latitudes, *Quarterly Journal of the Royal Meteorological Society*, 90, 441–466, doi:10.1002/qj.49709038607, 1964. 21301

Ribera, P., Peña-Ortiz, C., Garcia-Herrera, R., Gallego, D., Gimeno, L., and Hernández, E.: Detection of the secondary meridional circulation associated with the quasi-biennial oscillation, *J. Geophys. Res.*, 109, D18112, doi:10.1029/2003JD004363, 2004. 21295, 21301

Roscoe, H. K.: The Brewer-Dobson circulation in the stratosphere and mesosphere-Is there a trend?, *Adv. Space Res.*, 38, 2446–2451, 2006. 21293

Schoeberl, M. R., Douglass, A. R., Stolarski, R. S., Pawson, S., Strahan, S. E., and Read, W. G.: Comparison of lower stratospheric tropical mean vertical velocities, *J. Geophys. Res.*, 113, 24109, doi:10.1029/2008JD010221, 2008. 21294, 21296, 21300

Schwartz, M. J., Lambert, A., Manney, G. L., Read, W. G., Livesey, N. J., Froidevaux, L., Ao, C. O., Bernath, P. F., Boone, C. D., Cofield, R. E., Daffer, W. H., Drouin, B. J., Fetzer, E. J., Fuller, R. A., Jarrot, R. F., Jiang, J. H., Jiang, Y. B., Knosp, B. W., Krüger, K., Li, J.-L. F., Mlynchak, M. G., Pawson, S., Russell, J. M., Santee, M. L., Snyder, W. V., Stek, P. C., Thurstans, R. P., Tompkins, A. M., Wagner, P. A., Walker, K. A., Waters, J. W., and Wu, D. L.: Validation of the Aura Microwave Limb Sounder temperature and geopotential height measurements, *J. Geophys. Res.*, 113, D15S11, doi:10.1029/2007JD008783, 2008. 21296

Ueyama, R. and Wallace, J. M.: To What Extent Does High-Latitude Wave Forcing Drive Tropical Upwelling in the Brewer-Dobson Circulation?, *J. Atmos. Sci.*, 67, 1232–1246, doi:10.1175/2009JAS3216.1, 2010. 21293

Yulaeva, E., Holton, J. R., and Wallace, J. M.: On the Cause of the Annual Cycle in Tropical Lower-Stratospheric Temperatures, *J. Atmos. Sci.*, 51, 169–174, doi:10.1175/1520-0469(1994)051<0169:OTCOTA>2.0.CO;2, 1994. 21300

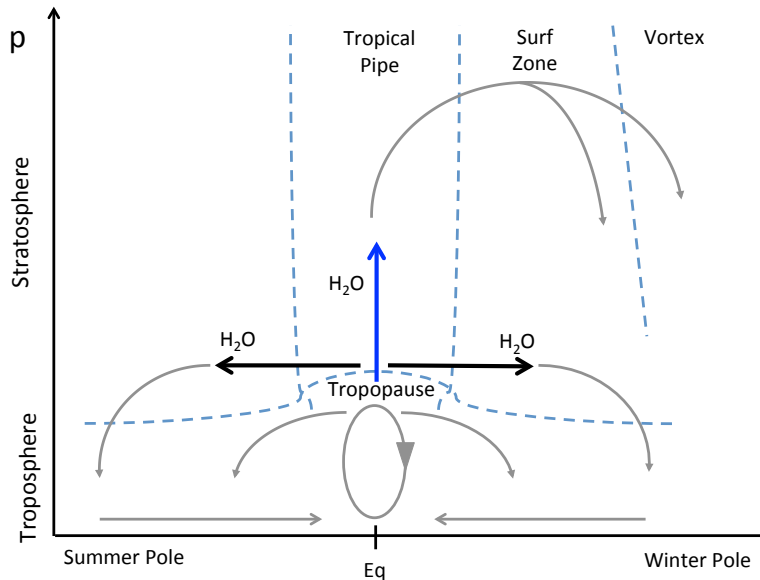


**Fig. 1.** Schematic of the Brewer-Dobson circulation in the stratosphere. In the lowermost stratosphere air is transported towards both poles (thick black arrows) before it reenters the troposphere at higher latitudes and is brought back to the tropics. The rising air masses in the tropics are transported towards the winter pole in the upper stratosphere, cross the tropical pipe and descend into the surf zone and the polar vortex. Breaking planetary waves drive the BDC and give the surf zone its name. Our study focuses on the three branches highlighted by the thicker blue and black arrows which distribute H<sub>2</sub>O in the stratosphere. The ellipse and the two poleward directed arrows represent the Hadley circulation in the troposphere.

**Variability of the Brewer-Dobson circulation**

T. Flury et al.

Title Page

Abstract Introduction

Conclusions References

Tables Figures

◀ ▶

◀ ▶

Back Close

Full Screen / Esc

Printer-friendly Version

Interactive Discussion



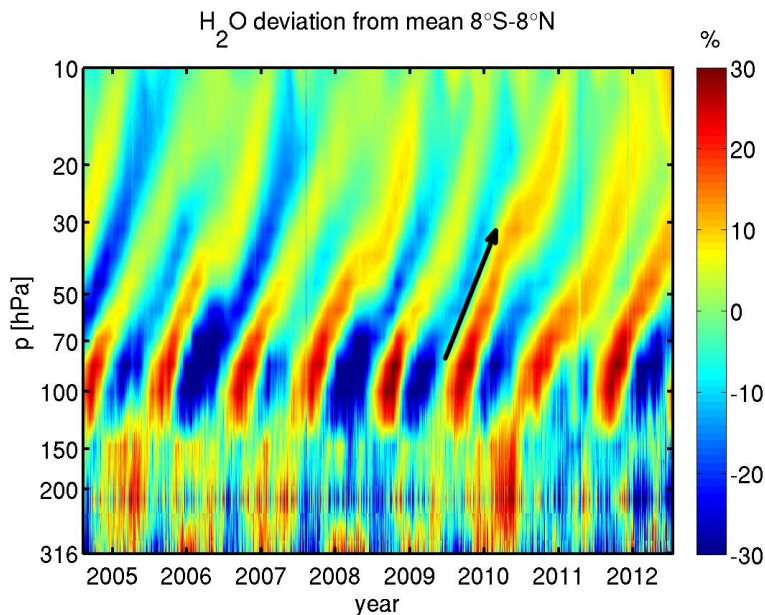


**Fig. 2.** The so called atmospheric tape recorder shows zonal mean  $\text{H}_2\text{O}$  anomalies in the tropics as a function of time and altitude. Red colors show above average volume mixing ratios whilst blue values show lower values mainly during NH winter. The seasonal cycle with an amplitude of about 30 % is imprinted at 100 hPa and slowly transported upward by the ascending branch of the BDC as indicated by the arrow. The slope of the arrow provides an indication of the average speed of the BDC. The variability between 316 and 150 hPa is mostly due to ENSO. In El Niño (La Niña) years more (less)  $\text{H}_2\text{O}$  is observed.

**Variability of the Brewer-Dobson circulation**

T. Flury et al.

Title Page

Abstract

Introduction

Conclusions

References

Tables

Figures

⏪

⏩

◀

▶

Back

Close

Full Screen / Esc

Printer-friendly Version

Interactive Discussion



## Variability of the Brewer-Dobson circulation

T. Flury et al.

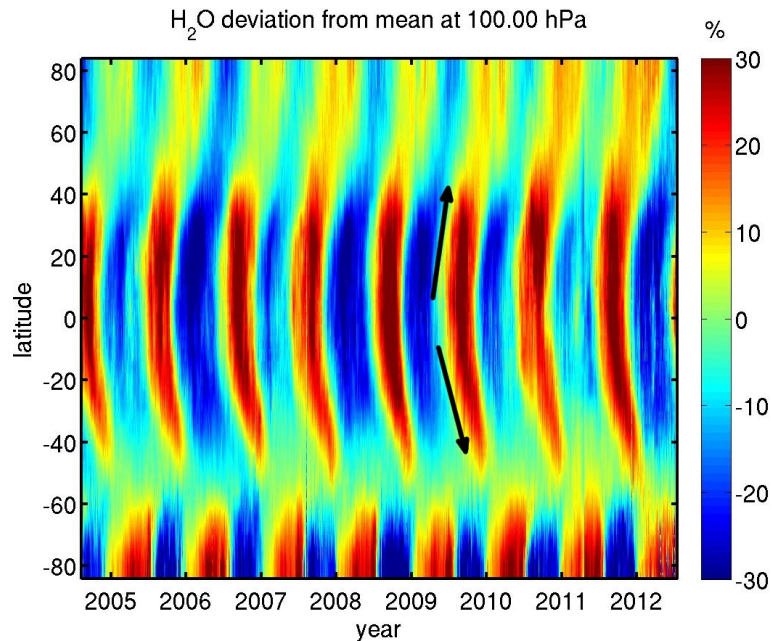


**Fig. 3.** Relative deviation from the average zonal mean H<sub>2</sub>O as a function of time and latitude at 100 hPa. Red colors show above average concentrations whilst blue values show lower values. The visible seasonal cycle with an amplitude of about 30% is transported from the tropics towards the poles by the meridional BDC as indicated by the arrows and can be identified along the slant lines of same colors. The slope is steeper towards the northern hemisphere which is due to a stronger and faster BDC.

[Title Page](#)[Abstract](#)[Introduction](#)[Conclusions](#)[References](#)[Tables](#)[Figures](#)[◀](#)[▶](#)[◀](#)[▶](#)[Back](#)[Close](#)[Full Screen / Esc](#)[Printer-friendly Version](#)[Interactive Discussion](#)

## Variability of the Brewer-Dobson circulation

T. Flury et al.

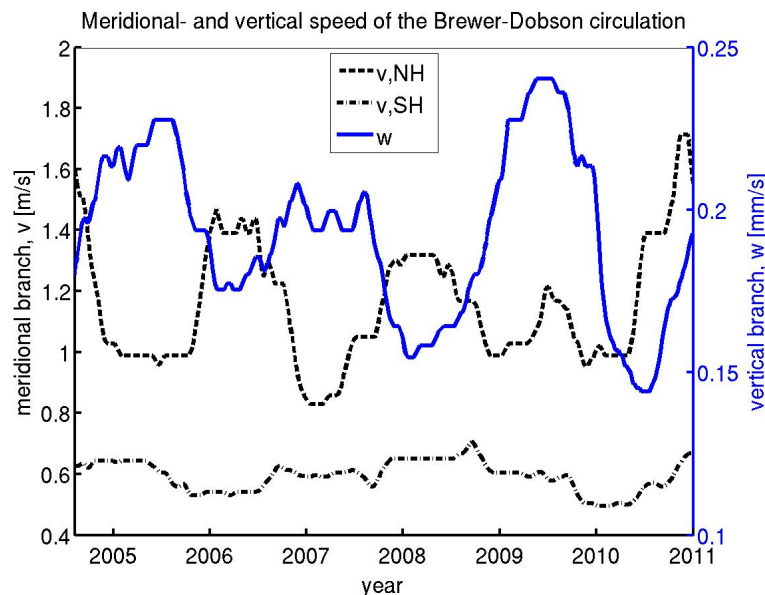


**Fig. 4.** Speed of the meridional branch of the BDC at 100 hPa to the NH ( $v$ , NH dashed black), to the SH ( $v$ , SH, dashdotted black) and the vertical branch ( $w$ , solid blue) at 68 hPa. Speeds show a prominent  $\sim 2$  yr oscillation related to the QBO. The meridional branch to the NH is about 5500 times faster than the vertical branch. Both  $v$ , NH and  $w$  show interannual variability of about 21 % with a period of a little more than two years. Generally the vertical speed increases in phase with a meridional speed decrease and vice versa. The speed to the SH shows less variability and is out of phase with the NH for the most part, except for the first 3 yr where they are correlated.

[Title Page](#)[Abstract](#)[Introduction](#)[Conclusions](#)[References](#)[Tables](#)[Figures](#)[◀](#)[▶](#)[◀](#)[▶](#)[Back](#)[Close](#)[Full Screen / Esc](#)[Printer-friendly Version](#)[Interactive Discussion](#)

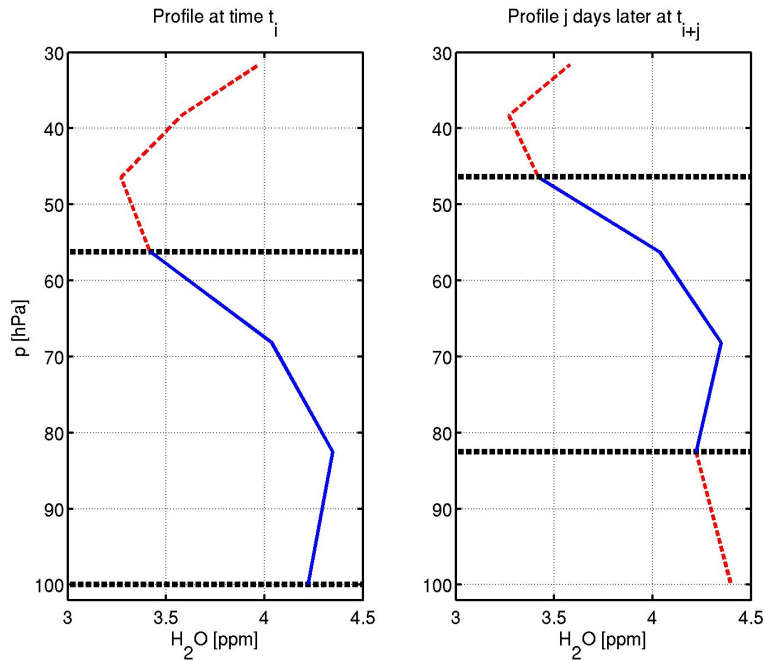


**Fig. 5.** Schematics on how the vertical ascent rate is computed using the same method as Niwano et al. (2003). A portion of a  $\text{H}_2\text{O}$  profile is taken at a time  $t_i$  between 100 hPa and 56 hPa, which is displayed on the left side in blue between the dashed horizontal lines. Due to BDC ascent the profile will be shifted upward some time later. At a specific time  $t_{i+j}$ ,  $j$  days later, the structure can be found one pressure level higher up, which is shown on the right. In order to compute this time, we correlate the blue  $\text{H}_2\text{O}$  segment on the left with the segment one level higher up on subsequent days until maximum correlation is reached after a time  $j$ . The ratio of the ascended distance and the time lag  $j$  yields the average ascent rate.

**Variability of the Brewer-Dobson circulation**

T. Flury et al.

Title Page

Abstract Introduction

Conclusions References

Tables Figures

◀ ▶

◀ ▶

Back Close

Full Screen / Esc

Printer-friendly Version

Interactive Discussion



**Variability of the  
Brewer-Dobson  
circulation**

T. Flury et al.

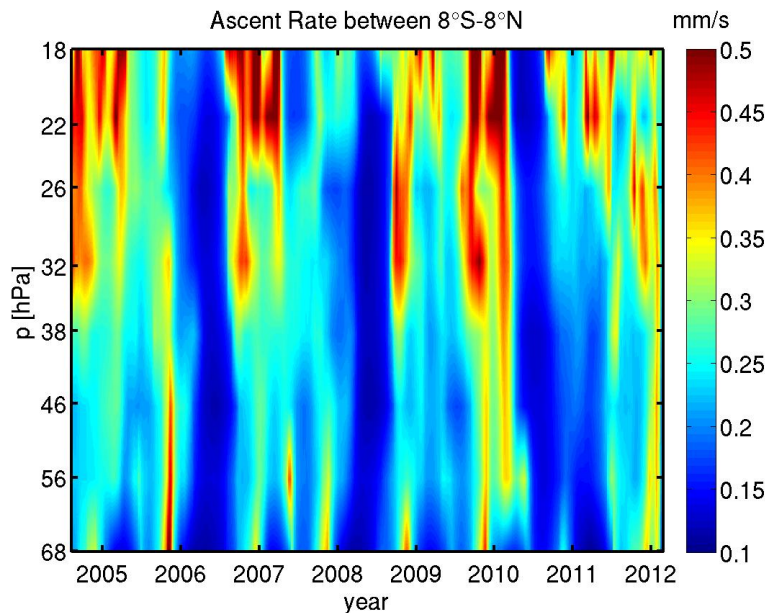


**Fig. 6.** Average vertical speed in the lower stratosphere between 68 hPa ( $\sim 18.8$  km) and 18 hPa ( $\sim 27.2$  km) as a function of time calculated according to Niwano et al. (2003). A seasonal cycle is apparent with higher speeds (red) increasing with altitude and towards the end of each calendar year during NH winter, which is consistent with the characteristics of the BDC that is strongest from September to March. During NH summer the vertical speed decreases (blue) due to the reduced planetary wave breaking, which is the main driver of the BDC.

Title Page

Abstract

Introduction

Conclusions

References

Tables

Figures

◀

▶

◀

▶

Back

Close

Full Screen / Esc

Printer-friendly Version

Interactive Discussion



## Variability of the Brewer-Dobson circulation

T. Flury et al.

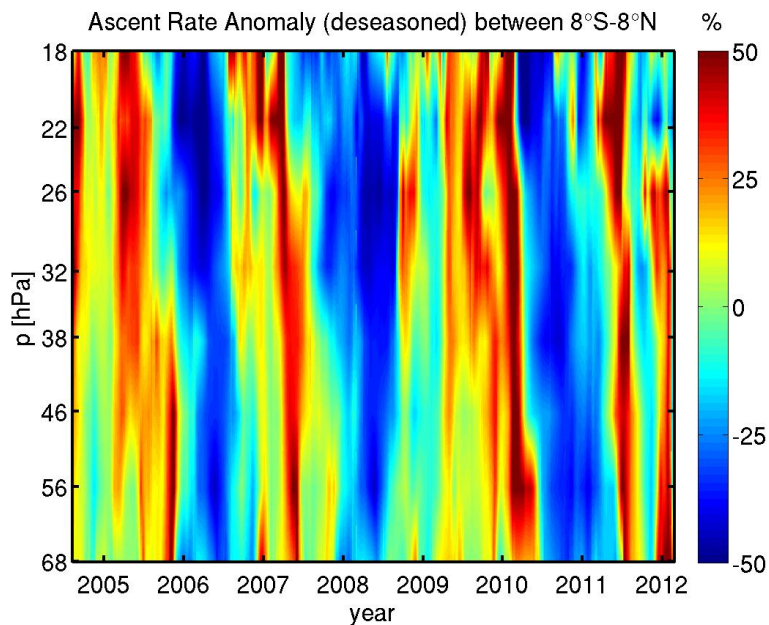


**Fig. 7.** Anomalies of the ascent rates shown in Fig. 6 with the seasonal cycle removed. A distinct  $\sim 2$  yr cycle is visible which is descending slowly at a rate of about  $1.5 \text{ km month}^{-1}$ . The variability is about 50% with lower ascent rates (blue) observed in 2006, 2008 and 2010-11. The negative anomalies occur during the QBO westerly phase as will be shown in Fig. 10.

Title Page

Abstract

Introduction

Conclusions

References

Tables

Figures

◀

▶

◀

▶

Back

Close

Full Screen / Esc

Printer-friendly Version

Interactive Discussion



## Variability of the Brewer-Dobson circulation

T. Flury et al.

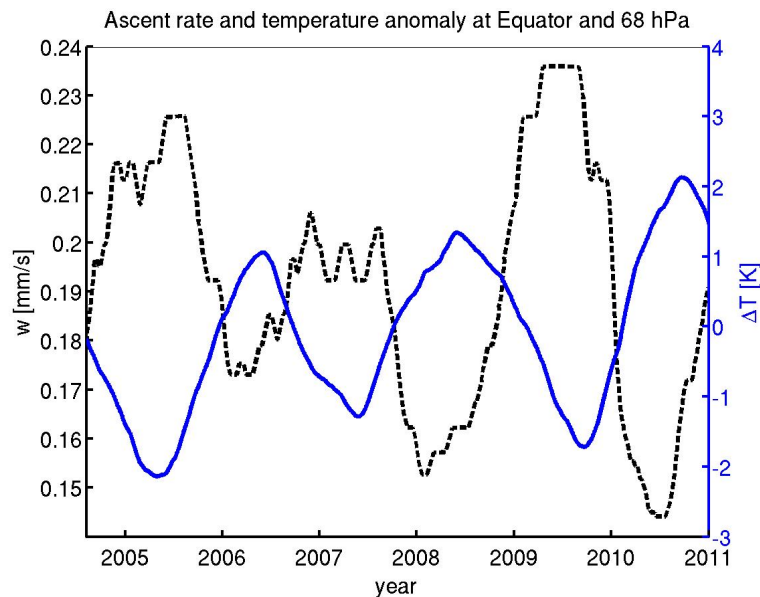


**Fig. 8.** The vertical ascent rate at the Equator between 68 hPa and 56 hPa (black dashed) is compared to the MLS temperature anomaly (blue solid) at the same latitude and altitude. The temperature time series has been smoothed by a one year forward moving average to match the method which is used to determine the ascent rate. Each value represents the average over the next year. Temperature anti-correlates with the vertical ascent as expected from theory.

[Title Page](#)[Abstract](#)[Introduction](#)[Conclusions](#)[References](#)[Tables](#)[Figures](#)[◀](#)[▶](#)[◀](#)[▶](#)[Back](#)[Close](#)[Full Screen / Esc](#)[Printer-friendly Version](#)[Interactive Discussion](#)

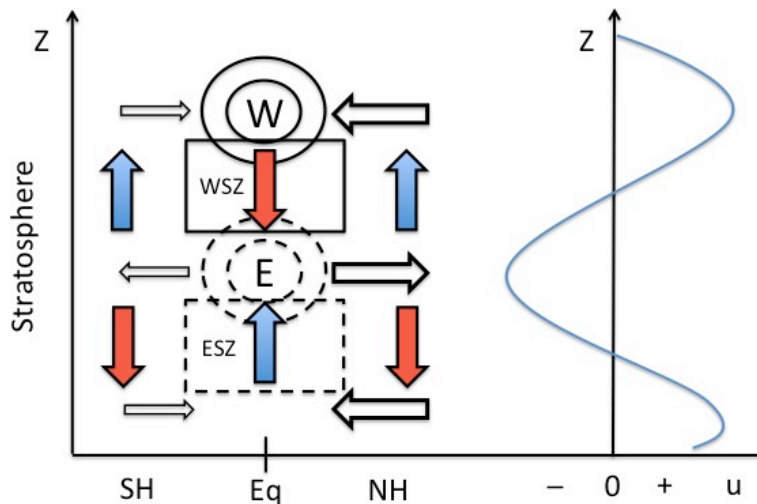


**Fig. 9.** Sketch of the QBO secondary meridional circulation on the left and the zonal wind profile at the Equator on the right. Arrows indicate vertical and meridional motion with colors meaning warming (red) and cooling (blue). Below the altitude of maximum easterlies (E) air is rising faster in the easterly shear zone (ESZ). At the altitude of maximum easterlies air is diverging towards the poles and increases the speed of the BDC, the opposite is found at the altitude of maximum westerlies (W) where air converges at the equator (Eq) and leads to downdrafts below that level which decrease the speed of the ascent and warm the atmosphere inside the westerly shear zone (WSZ). Figure adapted from Choi et al. (2002); Plumb and Bell (1982); Punge et al. (2009). From our results of the hemispheric asymmetry in the meridional BDC-branch we conclude that the secondary meridional circulation is less strong in the NH by a factor of 2 and reduced the SH arrows accordingly in size.

**Variability of the Brewer-Dobson circulation**

T. Flury et al.

Title Page

Abstract Introduction

Conclusions References

Tables Figures

◀ ▶

◀ ▶

Back Close

Full Screen / Esc

Printer-friendly Version

Interactive Discussion



## Variability of the Brewer-Dobson circulation

T. Flury et al.

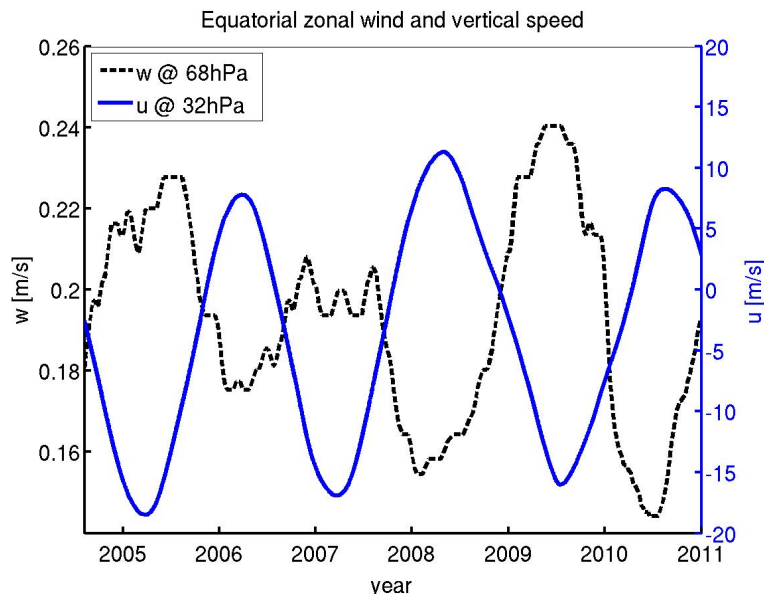


**Fig. 10.** Ascent rate  $w$  at the Equator between the 68 and 56 hPa level (dashed black) together with the average equatorial zonal wind  $u$  (solid blue) higher up at 32 hPa. In order to compare to the ascent rate the zonal wind is smoothed with a one year forward moving average. The data confirm the sketch in Fig. 9 and show maximum ascent rates during the easterly phase ( $u < 0$ ) and minimum during the westerly phase ( $u > 0$ ).

Title Page

Abstract

Introduction

Conclusions

References

Tables

Figures

◀

▶

◀

▶

Back

Close

Full Screen / Esc

Printer-friendly Version

Interactive Discussion



## Variability of the Brewer-Dobson circulation

T. Flury et al.

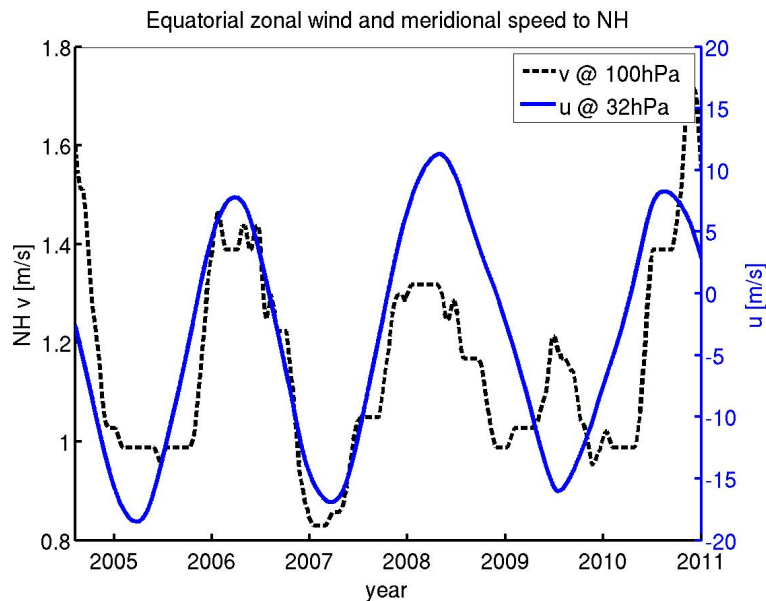


**Fig. 11.** Speed of the meridional branch (dashed black) of the BDC to the NH at 100 hPa and the average equatorial zonal wind at 32 hPa (solid blue, same as in Fig. 10). The meridional speed is in phase with the wind and increases (decreases) as suggested by Fig. 9 during the westerly/positive (easterly/negative) phase of the zonal wind.

[Title Page](#)[Abstract](#)[Introduction](#)[Conclusions](#)[References](#)[Tables](#)[Figures](#)[◀](#)[▶](#)[◀](#)[▶](#)[Back](#)[Close](#)[Full Screen / Esc](#)[Printer-friendly Version](#)[Interactive Discussion](#)

## Variability of the Brewer-Dobson circulation

T. Flury et al.

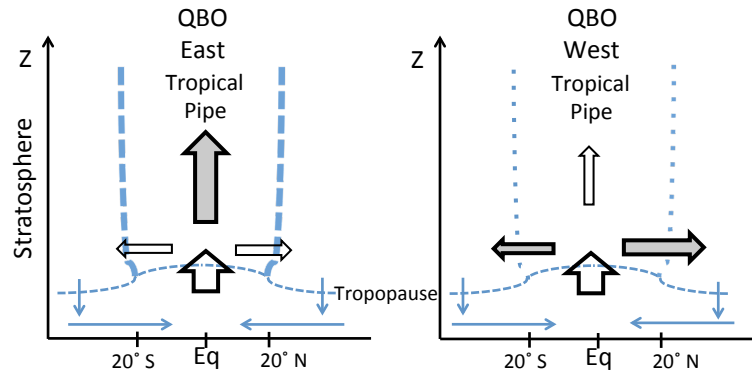


**Fig. 12.** Interpretation of the QBO influence on the BDC variability. During the QBO easterly phase on the left the tropical pipe is stronger and it takes more time for air masses to cross the barrier towards mid-latitudes. Thus the meridional speed is slower. For continuity, the vertical branch has to speed up which is shown by the big shaded vertical arrow. On the other hand during the QBO westerly phase the tropical pipe is more leaky and transport towards the mid-latitudes faster what is shown on the right. Again, for continuity reasons, the vertical transport has to slow down which agrees well with our results.

Title Page

Abstract

Introduction

Conclusions

References

Tables

Figures

◀

▶

◀

▶

Back

Close

Full Screen / Esc

Printer-friendly Version

Interactive Discussion

